

Original Article

The therapeutic potential of repurposed mebendazole, alone and in synergistic combination with ONC201, in the treatment of diffuse midline glioma

Serena Gentile¹, Federica Toma², Donatella Lucchetti^{2,3}, Lucia Lisi⁴, Pierluigi Navarra⁴, Alessandro Sgambato^{2,3}, Tiziana Servidei¹, Antonio Ruggiero^{1,5}

¹Pediatric Oncology Unit, Department of Woman and Child Health Sciences and Public Health, Fondazione Policlinico Universitario A. Gemelli IRCCS, 00168 Rome, Italy; ²Department of Translational Medicine and Surgery, Università Cattolica del Sacro Cuore, 00168 Rome, Italy; ³Fondazione Policlinico Universitario A. Gemelli IRCCS, 00168 Rome, Italy; ⁴Department of Healthcare Surveillance and Bioethics, Section of Pharmacology, Università Cattolica del Sacro Cuore - Fondazione Policlinico Universitario A. Gemelli IRCCS, 00168 Rome, Italy; ⁵Department of Life Sciences and Public Health, Università Cattolica del Sacro Cuore, 00168 Rome, Italy

Received February 7, 2025; Accepted April 10, 2025; Epub June 15, 2025; Published June 30, 2025

Abstract: H3K27-altered diffuse midline glioma (DMG) is a universally fatal disease with no available therapeutic strategies apart from palliative radiotherapy. Repurposing marketed non-cancer drugs in oncology is emerging as a fast-tracking approach to speed up the development of new treatment options, urgently needed for DMG. Repurposed anthelmintic mebendazole (MBZ) is in the spotlight against brain tumors, because it joins promising anticancer properties with high neuropenetrance, favorable pharmacokinetic and safety profile. Although MBZ is undergoing Phase I/II trials against brain tumors, including DMG, MBZ anticancer properties and the underlying mechanisms of actions have poorly been characterized in DMG preclinical models. We found that MBZ robustly reduced cell viability in six out of seven DMG cell lines with either K27M-mutated or wild-type H3. All IC₅₀ values (range 102 to 958 nM) fell in a clinically attainable range. The antiproliferative MBZ properties were mediated by an arrest of DMG cells in the G₂/M phase with a concomitant upregulation of the key cell cycle regulators p21 and p27, whereas p53 upregulation and activation were cell context-dependent. At the same growth-inhibitory concentrations, MBZ triggered apoptotic cell death, as evidenced by higher levels of the apoptotic markers caspase-3 and PARP cleavage. Consistently, Annexin V-Propidium iodide (PI) double staining showed MBZ dose-dependent increase in both stages of apoptosis. Of interest, the combination of MBZ with the first-in-class imipridone ONC201 synergistically increased the antiproliferative effects in two DMG cell lines as assessed by combination scores with different algorithms, showing additive effects in two others cell lines. Mechanistically, the combination potentiated the proapoptotic activity of either MBZ or ONC201, while not changing the cytokinetic perturbations induced by the single drugs. Finally, one pair of ONC201-sensitive and ONC201-resistant DMG cell lines with acquired resistance showed same responsiveness to MBZ with similar values of IC₅₀ and E_{max}. In conclusion, MBZ demonstrates high growth-inhibitory/proapoptotic activity, chemosensitization property to ONC201 and the ability to overcome ONC201 resistance in DMG cell cultures, proposing as a new low-toxicity therapeutic for DMG, with a potential to be used in second-line treatment and/or in combination protocols.

Keywords: Drug repurposing, mebendazole, diffuse midline glioma, ONC201, combination therapy, synergism, apoptosis, p53, cell cycle, H3 K27M mutation

Introduction

Diffuse midline gliomas (DMG) represent the leading cause of cancer-related mortality in children. According to the latest World Health Organization (WHO) classification of Central Nervous System (CNS) tumors, this group of

neoplasms are categorized as DMG H3 K27-altered based on global hypomethylation of lysine 27 of histone H3 (H3K27) as a driving force for spurious gene expression and uncontrolled tumor growth [1]. This epigenetic alteration results from two mutually exclusive mechanisms, that is H3 K27M-mutation occurring in

Mebendazole against diffuse midline glioma

the majority of DMGs and Enhancer of Zeste Homologs Inhibitory Protein (EZHIP) over-expression with wild-type H3 present in almost all the remaining tumors [1-3].

Due to location within vital areas of the midline structures of the brain and infiltrative nature, surgical resection of DMG tumors is extremely challenging, and focal radiotherapy (RT) is the only life-prolonging treatment. Such approach, however, shows a marginal influence on the course of disease as median overall survival (OS) is 9-11 months, and only 2% of children survive 5 years after diagnosis [4, 5]. Over 250 clinical trials spanning several decades and testing a vast array of therapeutic interventions, including cytotoxic chemotherapy, chemoradiation, molecularly targeted therapy and immunotherapy, have not improved patient outcomes [3]. Thus, new chemotherapeutic options are urgently needed to defeat these universally fatal tumors [6, 7].

In the recent years, drug repurposing - i.e. the use of already Food and Drug Administration (FDA) -approved drugs for indications other than their originally intended use - is emerging as a fast-tracking, cost-effective approach to expedite the developmental timelines of new therapeutic strategies [8, 9]. In this scenario, mebendazole (MBZ) has garnered interest as one of the most promising repurposed drugs against brain cancers [10-12]. It has shown more than 40 years of safe use in humans as an anthelmintic drug and serendipitously been discovered having anticancer properties against animal brain tumor models. In addition to its well-known destabilizing effects on microtubule polymerization of fast-dividing cells [13], MBZ inhibits a number of oncogenic signaling pathways and cancer-related cellular processes, such as angiogenesis and epithelial-to-mesenchymal transition, while triggering apoptosis and cell cycle arrest. In cultured glioblastoma (GBM) and medulloblastoma (MB) cell lines dosed with MBZ, the IC_{50} s for cell viability vary from 0.1 to 0.5 μ M [10, 14], concentrations that are clinically attainable [15]. *In vivo* administration of MBZ prolongs survival of mice bearing intracranial GBM [10] and MB [16], with concomitant reduction in vascularity in tumor, but not in normal tissues. Of interest, *in vitro* high-throughput screening testing large mechanistically annotated collections of approved

and investigational compounds have identified MBZ among the top potency-selected agents active against cell lines derived from childhood solid tumors [17], including DMG [18].

Therefore, due to its broad mechanisms of actions as anticancer agent and proven synergy with chemotherapy and RT in the preclinical setting, as well as its high blood brain barrier penetrability and favorable pharmacokinetic and safety profile in the clinical setting, MBZ meets many of the ideal features for a repurposed drug for the treatment of CNS tumors [12, 19, 20]. Indeed, Phase I/II clinical trials are currently undergoing in both adults (NCT01729260) and children (NCT02644291, NCT01837862) to investigate the anticancer effect of MBZ, alone or in combination with standard chemotherapy drugs, for the treatment of brain tumors including DMG. Moreover, computational multiomics-based approaches used for biomarker-guided drug selection have identified MBZ as one of the medicines of choice for personalized treatments of patients with DMG to block specific signaling [21] or in backbone therapies [22].

However, thorough mechanistic investigations of the anticancer properties of MBZ in DMG cell cultures has not been performed. A deeper knowledge of the cellular and molecular processes underlying the antitumor effects of MBZ and of its pharmacological interactions with other agents are essential for the inclusion of MBZ in more efficacious treatment protocols against DMG [11]. Emerging evidence shows that DMGs display large intertumoral and intratumoral heterogeneity, highlighting the need for combination therapies to overcome clonal diversity and the occurrence of resistance.

With these premises, we characterized the effects of MBZ across a panel of DMG H3K27M-mutated and H3 wild-type cell lines, by utilizing cell survival analyses, cell cycle profiling and markers of cell death. In addition, we performed combination experiments to investigate MBZ's role in chemosensitizing DMG cells to ONC201, a promising investigational compound that is currently in advanced phase clinical trials against H3K27-altered gliomas showing preliminary survival benefits [3]. Finally, the ability of MBZ to overcome ONC201 resistance is highlighted.

Mebendazole against diffuse midline glioma

Materials and methods

Cell culture and reagents

Primary DMG cell culture models (SU-DIPG-VI(E), SU-DIPG-XIII-FL, SU-DIPG-XIII-P*, SU-DIPG-XLVIII, SU-DIPG-XXXVIII) were kindly provided by Dr. Michelle Monje, Stanford University. SF8628 and SF7761 were purchased from Merck Millipore (Burlington, MA, USA). SF8628 cells were maintained in Dulbecco's modified Eagle medium (DMEM) High glucose (Euroclone) supplemented with 10% fetal bovine serum (FBS) and GlutaMAX-I (Thermo Fisher, Invitrogen brand, Carlsbad, CA, USA) and grown in adherent culture conditions. All the other cell lines were grown in tumor stem serum-free media, made up of Neurobasal-A medium and DMEM/F-12 1:1, N-(2-Hydroxyethyl)piperazine-N'-(2-ethanesulfonic acid) (HEPES) buffer, sodium pyruvate, minimum essential medium (MEM) nonessential amino acids, antibiotic-antimycotic solution, GlutaMAX-I, B-27 supplement minus vitamin A (all purchased from ThermoFisher), supplemented with human fibroblast growth factor 2 (FGF2), human epidermal growth factor (EGF), human platelet-derived growth factor A (PDGFA), human platelet-derived growth factor B (PDGFB) (from Shenandoah Biotechnology Inc., Warwick, PA, USA), and 0.2% Heparin (STEM-CELL Technologies, Vancouver, BC, Canada).

The ONC201-resistant variant, referred to as SU-DIPG-XIII-R, was established by continuous exposure of the parental line to stepwise increasing ONC201 concentrations and maintained in a medium always containing 0.7 μ M of the selecting agent.

MBZ (HY-17595, CAS No 31431-39-7, Polymorph C) and ONC201 (CAS No 1616632-77-9) were purchased from MedChemExpress (LLC, Monmouth Junction, NJ, USA), and dissolved in dimethyl sulfoxide (DMSO) to a stock concentration of 10 mM. Serial dilutions were made in cell culture media prior to cell treatments.

Cell viability assay

All suspension cell lines were plated in 96-well plates at a density of 5000 cells/well, whereas SF8628 were plated at a density of 1000 cells/well. After 24 hours, the cells were treated with vehicle DMSO or serial dilutions of each drug in

triplicate or quadruplicate for 72 hours. Cell viability was determined by CellTiter-Glo (CTG, Promega, Madison, WI, USA) and bioluminescence imaging was measured using the TECAN imaging system (Tecan Spark, Tecan Austria GmbH Grödig, Austria). The half maximal inhibitory concentration (IC_{50}), the 95% confidence interval (95% CI) and maximal effect (E_{max} , defined as the cell proliferation inhibition percentage at the highest dose) were calculated using the sigmoidal dose-response function (variable slope, four parameters) of data with the GraphPad Prism version 8.00 for Windows (GraphPad Software Inc., San Diego, CA, USA).

Cell numbers of live and dead cells were assessed by an automated cell counter (NucleoCounter 100TM, ChemoMetec, Allerød, Hovedstaden, Denmark), that discriminates between live and dead cells through staining of nuclei with propidium iodide.

Drug combination and synergy assessment

For combination drug testing, cells were treated with each drug as a single-agent or in combination for 72 hours and cell viability was evaluated using the CellTiter-Glo assay. The pharmacological interaction between MBZ and ONC201 was calculated using the Compusyn software (ComboSyn, Inc.) and expressed as Combination Index (CI) based on the Chou - Talalay median-effect equation method, where a CI value < 1 is synergistic and a CI > 1 indicates antagonism [23].

To avoid biased synergy estimation, we also used the SynergyFinder 3.0 free web-application [24], which enables to quantify the combinatorial effects with multiple synergy reference models, each of them formulated under different assumptions of single-drug behavior, including Bliss excess, Loewe additivity, highest single-agent (HSA) and zero interaction potency (ZIP) [24, 25]. The conventional metrics are: antagonism < -10 ; additivity, from -10 to 10 ; synergism > 10 .

Flow cytometry

Cells were seeded at the appropriate concentrations to maintain them in a proliferative phase throughout the experiment. After 24 hours, cells were challenged with either vehicle or drug(s) at designated concentrations for 72

Mebendazole against diffuse midline glioma

hours. At the end of the treatment period, the cells were collected, dissociated and then filtered using Cell Strainer (EASYstrainer 70 μm , Greiner Bio-One, Kremsmünster, Austria). Thereafter, cells were resuspended and fixed adding ice-cold 80% Ethanol dropwise while vortexing and stored at 4°C. At the moment of analysis, fixed cells were stained using a cell cycle kit according to the manufacturer's instructions (Beckman coulter). After 15 minutes incubation at room temperature and protected from direct light exposure, fluorescence of treated and control samples was measured with flow cytometry (CytoFLEX S, Beckman Coulter, Milan, Italy).

Western blotting

SU-DIPG-XLVIII and SF8628 were seeded in the appropriate vessels and challenged 24 hours later with drug(s) at the designated concentrations for different time intervals. Vehicle-treated cells were used as controls. At the end of the treatment period, the cells were harvested, washed with ice-cold phosphate buffered saline (PBS) and disrupted in Pierce RIPA buffer with Halt Protease inhibitor cocktail (Thermo Fisher Scientific). Cell lysates (15 $\mu\text{g}/\text{lane}$) were resolved by precast SDS-PAGE gel (Bio-Rad Laboratories, Inc., Hercules, CA, USA) and transferred to a nitrocellulose membrane. The membranes were probed with the following primary antibodies overnight at 4°C: phospho-p53 (S15) (9284S, 1:1000), p21 Waf1/Cip1 (12D1) (2947S, 1:1000), cleaved Caspase 3 (Asp175) (5A1E) (9664, 1:1000), GAPDH (5174, 1:1000), all from Cell Signaling Technology (Danvers, MA, USA); p53 (DO-1) (sc-126, 1:1000), p27 Kip-1 (F-8) (sc-1641, 1:500) and cleaved PARP (Sc-56196, 1:1000) were from Santa Cruz Biotechnology, Dallas, TX, USA. All blots were incubated with the corresponding secondary horseradish peroxidase conjugated anti-mouse IgG (PI-2000, 1:10000) or anti-rabbit IgG (PI-1000, 1:10000) from Vector Laboratories (Newark, CA, USA). Immunoreactive bands were developed by enhanced chemiluminescence (ECL prime, GE Healthcare, Amersham, United Kingdom). Densitometry analysis of the bands was performed using the Image Lab software version 6.0.1 (Bio-Rad Laboratories Inc., Hercules, CA, USA).

Apoptosis

Cell apoptosis analysis was performed by treating appropriate numbers of SU-DIPG-XLVIII ($1 \times$

10^6) and SF8628 (0.25×10^6) cells with different drug(s) concentrations for 72 hours. At the end of the incubation period, the samples were collected, dissociated in single cells and stained with the Dead Cell Apoptosis Staining kit (Thermo Fisher Scientific) containing Fluorescein isothiocyanate (FITC) - Annexin V conjugates and propidium iodide (PI), according to the manufacturer's instructions. After incubation in the dark for 15 minutes at room temperature, the fluorescence of the treated samples was measured with flow cytometry (CytoFLEX S, Beckman Coulter, Milan, Italy).

Results

MBZ restrains the proliferation of DMG cells

We evaluated the antiproliferative effects of MBZ in 7 cell cultures of DMG representing neurosphere (SU-DIPG-XIII-FL, SU-DIPG-VI, SU-DIPG-XLVIII, SU-DIPG-XIII-P*, SF7761) and adherent models (SF8628 and SU-DIPG-XXXVIII). SU-DIPG-XIII-P* and SU-DIPG-XIII-FL (the latter indicated thereafter as SU-DIPG-XIII) have been derived from the primary pontine tumor and the secondary frontal lobe lesion from the same patient, respectively [26, 27]. The DMG panel encompasses the complete genetic background of the tumor, including lines with H3.1K27M (SU-DIPG-XXXVIII), wild-type H3 (SU-DIPG-XLVIII), and the hallmark mutation H3.3K27M (all the remaining lines). Cytotoxicity was assessed after 72 hours of exposure to increasing MBZ concentrations (from 50 to 5000 nM) by the CTG assay. Dose-dependent response to MBZ was observed in 6 out of 7 DMG lines, with IC_{50} values spanning from 102 nM to 958 nM. The median IC_{50} was 290 nM, whereas the median value of E_{max} (%), indicating the maximum effect corresponding to the minimum measured viability [28], was 71% (range: 58 to 82%) (**Figure 1A, 1B**). SU-DIPG-VI cells were the less responsive to MBZ, yielding the lowest E_{max} (35%). Importantly, the IC_{50} values that we found *in vitro* are attainable in a clinical range [15]. For example, in a recent Phase 1 dose-escalation study in patients with high-grade glioma, plasma concentrations of MBZ reached 1 μM with long-term safety and acceptable toxicity [29].

To further characterize the pharmacological efficacies of MBZ, we determined cell viability and cell death by cell counting in SU-DIPG-XLVIII

Mebendazole against diffuse midline glioma

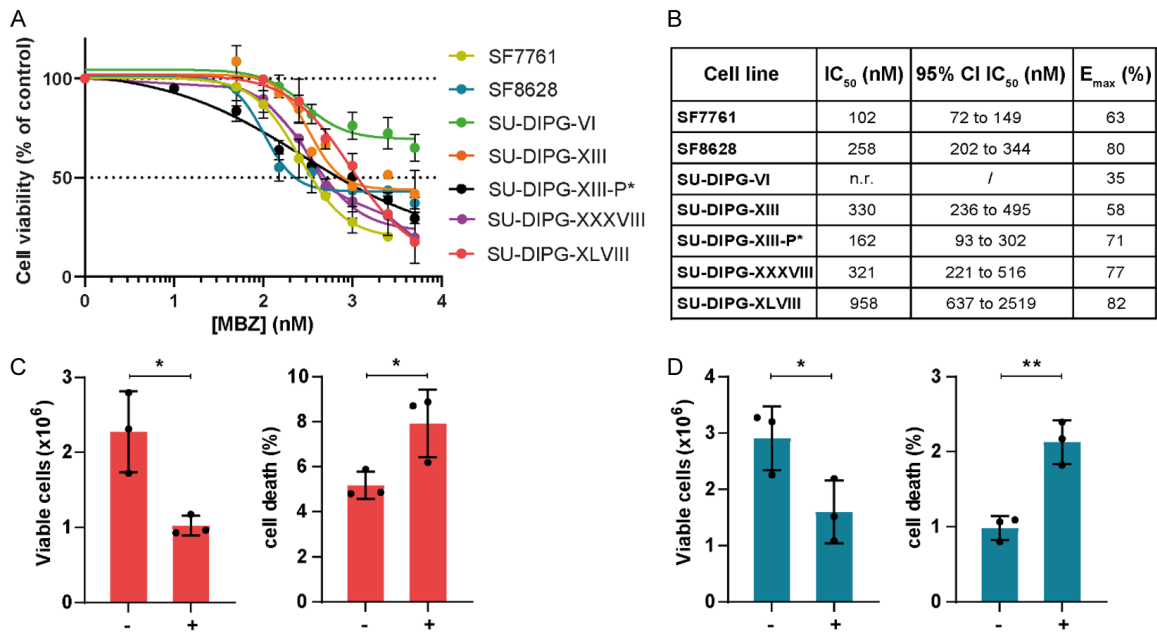


Figure 1. MBZ reduces cell viability of DMG cell lines. (A) Dose-response curves and IC₅₀ graphic representation (dotted line) of MBZ effects on the indicated DMG cell lines. Cell viability was measured by CTG assay after 72 hours drug exposure. Results represent cell viability percentage respect to vehicle-treated control cells for three independent experiments performed in triplicate (mean ± SE). (B) IC₅₀ values with 95% confidence intervals and E_{max} (%). Cell viability and cell death (%) in the SU-DIPG-XLVIII (C) and SF8628 (D) cell lines at equitoxic doses of MBZ as determined by cell counting. Cells were treated with the corresponding IC₅₀ (1 μM and 0.25 μM, respectively) for 72 hours, when viable and non-viable cells were counted by NucleoCounter. Each bar represents the mean ± SD from three independent experiments (*P < 0.05; **P < 0.01; mean ± SD; two-tailed Student's t test). n.r.: not reached.

(Figure 1C) and SF8628 (Figure 1D), that exhibited different sensitivities to MBZ in terms of IC₅₀ (1 μM and 0.25 μM, respectively), but high and comparable E_{max} values (82 and 80%, respectively). Recently, growing evidence has shown that DMG with wild-type and K27M-mutated H3 have different epigenomic and transcriptional landscapes, and possible differences in therapeutic strategies [30], advocating focused preclinical characterization of their chemosensitivity profile. MBZ concentrations equal to the respective IC₅₀ values determined a reduction in viable cell number by about 50% in both lines as expected, that was accompanied by a two-fold increase in the number of non-viable cells. All the subsequent experiments were performed at these equitoxic concentrations of MBZ, unless otherwise specified.

MBZ induces perturbations of cell cycle in DMG cells by targeting cell checkpoint proteins p21 and p27

To determine the contribution of cytostasis vs apoptosis in the reduction in cell number

induced by MBZ, we evaluated the perturbations of cell cycle in SU-DIPG-XLVIII and SF8628 cultures after exposure to the corresponding IC₅₀ for 24, 48 and 72 hours. Overall, the alterations of cytokinetic profile induced by MBZ were similar in the two lines, although of different entity: in SU-DIPG-XLVIII, an almost two-fold accumulation of cells in the S and G2/M phases was observed as soon as 24 hours of drug exposure (Figure 2A), that further increased at 48 hours and persisted up to 72 hours, with a concomitant marked reduction in the G0/G1 population at the corresponding time points. In the SF8628 line, changes in the cell cycle distribution were globally modest (Figure 2B), being an increase in the G2/M compartment at 24 hours up to 72 hours the most overt effect.

Parallel Western blotting experiments carried out upon identical experimental conditions showed that MBZ upregulated the expression of the tumor suppressor proteins p53 and p21 in a time-dependent manner in SU-DIPG-XLVIII and this effect was already evident after 24 hour - exposure, whereas a frank increase in p27 protein level was observed at 48 hours to

Mebendazole against diffuse midline glioma

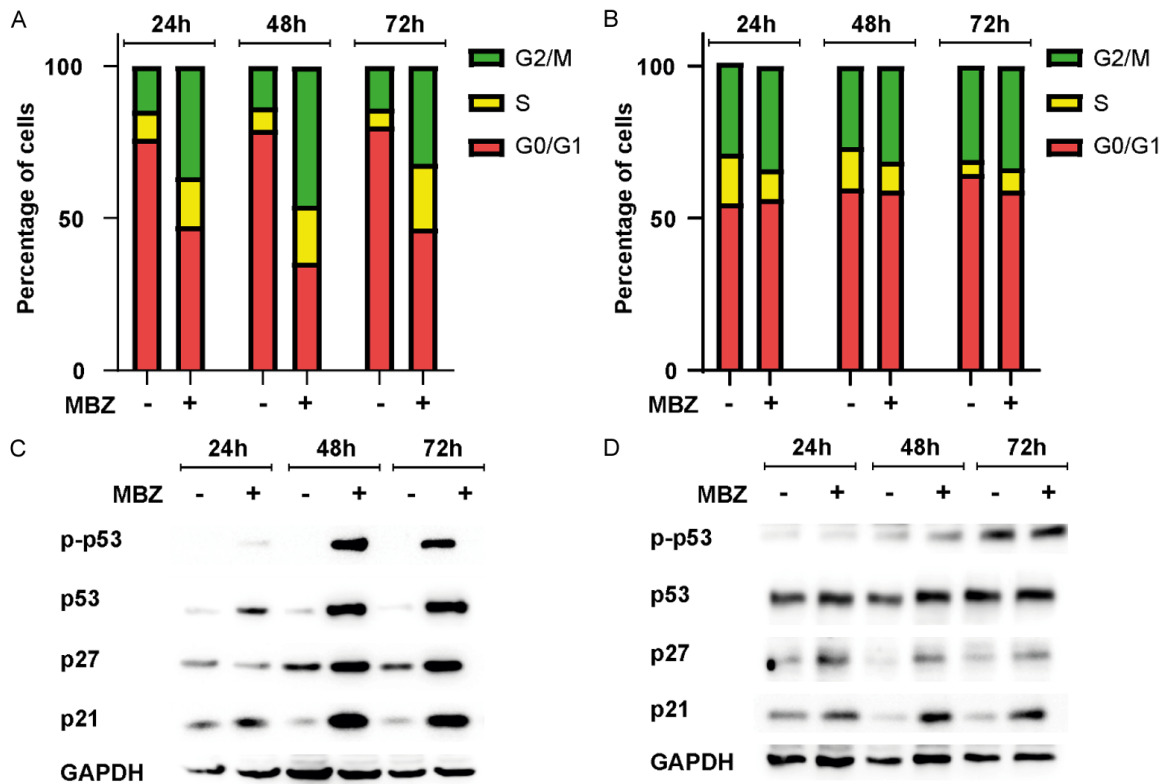


Figure 2. MBZ alters the cell cycle progression and the expression of regulatory proteins p53, p27 and p21. (A, B) Time-course analysis of the effects of MBZ on cell cycle distribution in SU-DIPG-XLVIII (A) and SF8628 (B) cell lines. Cells were treated with MBZ at the respective IC_{50} (1 μ M and 0.25 μ M, respectively) for the indicated periods of time. The percentages of the total cell population in the different phases of the cell cycle were assessed by flow cytometry. (C, D) Western blot analysis of total lysates from SU-DIPG-XLVIII (C) and SF8628 (D) treated with vehicle or equitoxic doses (IC_{50}) of MBZ for 24, 48 and 72 hours. Blots were probed with the indicated antibodies. GAPDH was used as a loading control.

peak thereafter. Phosphorylation of p53 at Ser 15 was consistent with p53 modulation, suggesting that MBZ promotes p53 transcription factor activity, likely leading to the upregulation of the checkpoint proteins (i.e. p21) and cell cycle arrest (Figure 2C) [31]. In SF8628, carrying a mutation in the TP53 gene [32], p27 and mostly p21 showed a mild, time-dependent upregulation (Figure 2D), whereas there was no modulation of p53 nor of its activated form, in agreement with the little cell cycle changes observed. Thus, MBZ appears to block DMG cells at G2/M phase, regardless of their p53 status, although the effects on cell cycle are more evident in the presence of wild-type p53.

MBZ triggers apoptotic cell death in DMG cells

Next, we analyzed MBZ-induced caspase 3 activation and poly (ADP-ribose) polymerase (PARP) cleavage, two hallmarks of the apoptotic machinery. Both markers increased time-

dependently in the two MBZ-treated lines as soon as 24 hours (Figure 3A, 3B), indicating an early onset of the apoptotic process. To further investigate the mechanisms of cell death set in motion by MBZ, we used Annexin V-PI double staining to distinguish early from late apoptotic and necrotic cells after drug challenging of SU-DIPG-XLVIII (Figure 3C) and SF8628 (Figure 3D) at their IC_{25} s (500 nM and 100 nM, respectively) and IC_{50} s for 72 hours. MBZ potently induced both stages of apoptosis dose-dependently in the two lines, which showed different sensitivity: at the highest equitoxic dose, apoptotic cells were approximately 10-fold and 4-fold more in MBZ-treated SU-DIPG-XLVIII and SF8628 cultures, respectively, compared to the corresponding control cells.

Combinations of MBZ and ONC201 show synergistic activity against DMG

MBZ has been shown to act synergistically with drugs with different mechanisms of actions,

Mebendazole against diffuse midline glioma

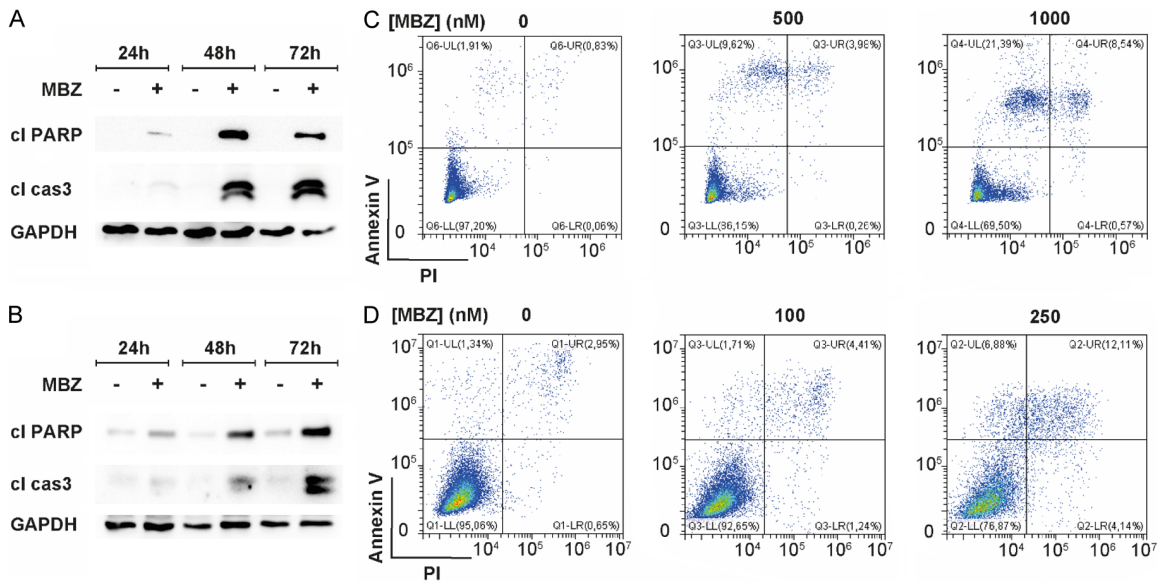


Figure 3. MBZ triggers apoptotic cell death in DMG cells. (A, B) Time course of the effects exerted by MBZ on the cleavage of PARP and the activation of caspase 3 in SU-DIPG-XLVIII (A) and SF8628 (B). Cells were exposed to equitoxic concentrations (IC_{50}) of MBZ for 24, 48 and 72 hours. Cell lysates were subjected to immunoblot analysis with the indicated antibodies. (C, D) Flow cytometry analysis of MBZ-treated SU-DIPG-XLVIII (C) cells and SF8628 cells (D) stained with annexin V-FITC and PI. Cells were incubated with vehicle or equitoxic concentrations (IC_{25} and IC_{50}) of MBZ for 72 hours.

including alkylating and molecularly-target agents [11, 19]. So far, no study has thoroughly addressed the combinatorial effects of MBZ with ONC201, a promising investigational compound that is currently in advanced phase clinical trials against DMG and other cancers [33]. Initially designed as a bitopic antagonist of dopamine receptor D2/3, ONC201 has subsequently been found to activate the mitochondrial caseinolytic protease P (ClpP) [3, 34] and to exert antineoplastic activity in different cancer models [35].

Because of the distinct mechanisms of action of MBZ and ONC201, we hypothesized that their combination could likely be synergistic. To examine the interaction between these two compounds, we firstly generated drug-response curves for ONC201 alone and in combination with a sub IC_{50} MBZ across four representative patient-derived DMG cell cultures namely SU-DIPG-XLVIII, SF8628, SU-DIPG-XIII-P* and SU-DIPG-XIII. All combinations were tested for 72 hours before assessment of cell viability. Encouragingly, ONC201 demonstrated a shift to the left of the dose-response curve in the four lines when combined with a low-dose of MBZ (Figure 4). Together these data suggest

increased efficacy of ONC201 when combined with MBZ.

Next, as a follow-up confirmatory screen, we performed a checkerboard assay, in which various concentrations of each drug were tested in duplicate both alone and in combinations for 72 hours. Each plate contained 6×5 -dose matrix dilutions of MBZ and ONC201. Overall, cell viability in each culture was reduced when the two compounds were used in combination rather than as monotherapy (Figure 5A). Combination analyses with the CalcuSyn 2.0 software (Biosoft) demonstrated consistent synergy ($CI < 1$) between MBZ and ONC201 across doses of drug combination and cell lines (Figure 5B).

We further validated the combination efficacy of MBZ with ONC201 by taking advantage from the Web application SynergyFinder, that allows to calculate and compare synergy scoring with four different reference models: HSA, Loewe, Bliss and ZIP [25, 36]. MBZ/ONC201 combination was synergistic in SU-DIPG-XLVIII (Figure 6A) and SF8628 (Figure 6B) when assessed by all the algorithms (score > 10). Instead, in SU-DIPG-XIII-P* (Figure 6C) and SU-DIPG-XIII

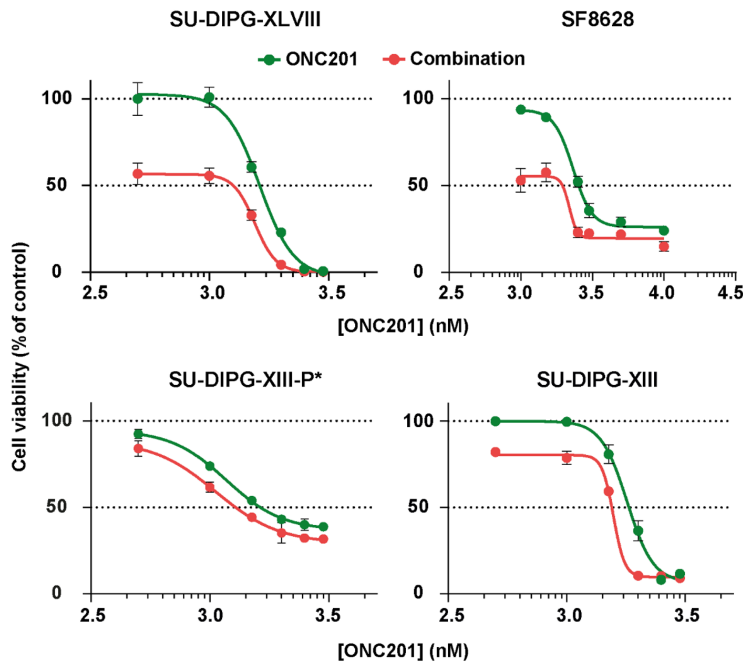


Figure 4. Low doses of MBZ potentiates the antiproliferative effects of ONC201. Dose-response curves of cell viability of DMG cell cultures after 72-hour exposure to ONC201 alone (green line) or with sub- IC_{50} of MBZ (red line). Cell viability was measured by CTG assay and expressed as percentage respect to vehicle-treated control cells. MBZ concentrations were as follows: 500 nM for SU-DIPG-XLVIII, 100 nM for all the other lines.

(**Figure 6D**) additivity was consistently found across all the models (score -10 to 10), with the exception of a Loewe score of 18.56 in SU-DIPG-XIII-P*, and a HSA score of 13.65 in SU-DIPG-XIII showing strong synergistic interaction. In the 2D synergy maps, algorithms identified the dose regions with the highest synergy score (highlighted by a white frame), that, in our case, corresponds to doses around the respective IC_{50} value of each drug in the different lines. For this reason, these IC_{50} values were selected for subsequent molecular studies.

Cotreatment with ONC201 potentiates the proapoptotic effects of MBZ in DMG cell lines

We next wondered whether the synergism between MBZ and ONC201 was mediated by an increase in cytostasis, in apoptosis or in both mechanisms. To this end, SU-DIPG-XLVIII cells were treated for 72 hours at doses of MBZ and ONC201 that resulted in the highest synergy score. FACS analysis revealed that the percentage of cells in the G2/M phase was even lower after co-treatment with MBZ-ONC201 than after treatment with

the most effective single-drug agent, that is MBZ alone (**Figure 7A**). Concordantly, MBZ and MBZ+ONC201 augmented the expression of p53 and p27 proteins to a similar extent, being the MBZ-induced p27 and p21 upregulation even reversed by the combination (**Figure 7B**). Importantly, MBZ+ONC201 induced the cleavage of PARP and of caspase 3 much more than either agent alone (**Figure 7C**). Similar data were obtained through the Annexin V-PI double staining, that showed that co-treatment markedly increased the percentage of apoptotic cells compared to monotherapy, while minimally affecting the proportion of necrotic cells (**Figure 7D**).

MBZ overcomes ONC201 resistance in DMG cells

ONC201 has been proved to be beneficial in early phase trials (NCT03416530 and NCT03134131) in pediatric patients with H3 K27M-mutant DMG [37]. However around 20-30% of patients with non-recurrent DMG show disease progression, suggesting that intrinsic or acquired resistance to ONC201 often occurs in clinical use.

To ascertain whether MBZ can be used in second-line therapy when upfront treatment with ONC201 fails, we evaluated the growth-inhibitory effects of ONC201 and MBZ in parental and ONC201-selected (SU-DIPG-XIII-R) cell lines. In this line, ONC201 resistance was associated with lower levels of the ONC201 target ClpP (**Figure 8A**, inset). ONC201 treatment for 72 hours demonstrated an IC_{50} of 1.497 μ M in SU-DIPG-XIII cells, in line with the literature data [38]. By contrast, IC_{50} was not reached in SU-DIPG-XIII-R treated with the same doses of ONC201, and E_{max} value was 32% as opposed to 72% in parental cells (**Figure 8A**). Of interest, sensitivity to MBZ was unaltered in the two lines as evidenced by similar values of IC_{50} and E_{max} , suggesting that MBZ overcomes acquired resistance to ONC201 (**Figure 8B**).

Mebendazole against diffuse midline glioma

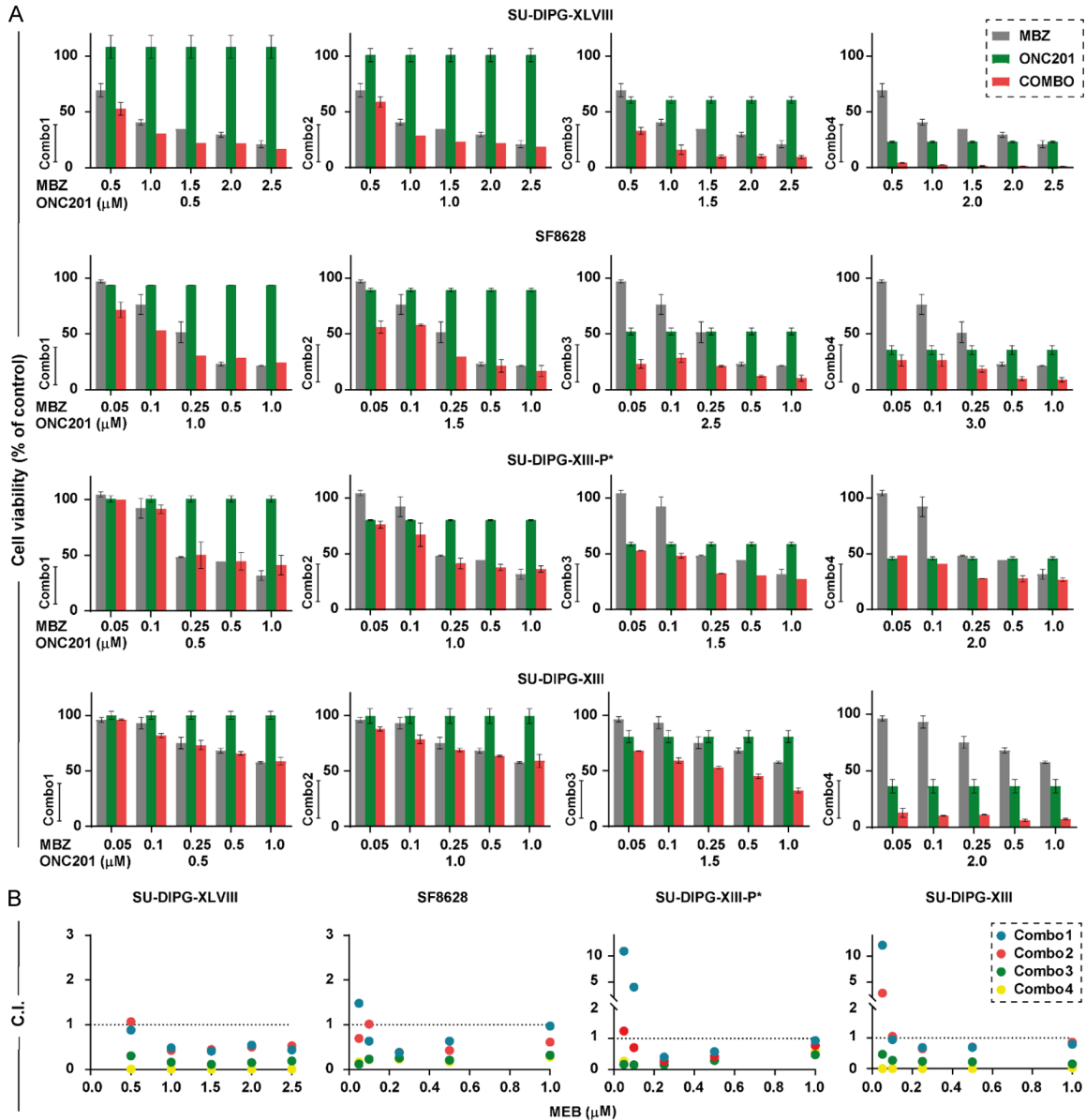


Figure 5. Combinations of MBZ and ONC201 show synergistic activity against DMG cells. (A) Cell viability compared to DMSO control after 72-hour exposure of four patient-derived DMG cell cultures to increasing doses of MBZ (grey), ONC201 (green), or both (red). (B) Synergy CI scores (CompuSyn 2.0) across doses for MBZ/ONC201 combinations from the individual viability measurements in (A). Horizontal dotted line indicates a CI = 1, where points below the line indicate synergy and points above the line indicate antagonism.

Discussion

Non-cancer medicines repurposed in oncology are emerging as an alternative approach to improve treatment protocols by reducing toxicity, enhancing efficacy and antagonizing drug resistance [39].

In search of novel and more effective therapeutic strategies for children with DMG, we investi-

gated the multifaceted therapeutic potential of repurposed anthelmintic MBZ in DMG cell lines. We show that MBZ restrains cell proliferation in DMG cell lines by both reducing cell cycle progression and triggering apoptotic cell death. Previously, high-throughput drug screening of 2706 investigational and marketed compounds targeting 860 distinct cellular mechanisms uncovered that MBZ was one of the 371 most potent agents against 4 DMG cell lines

Mebendazole against diffuse midline glioma

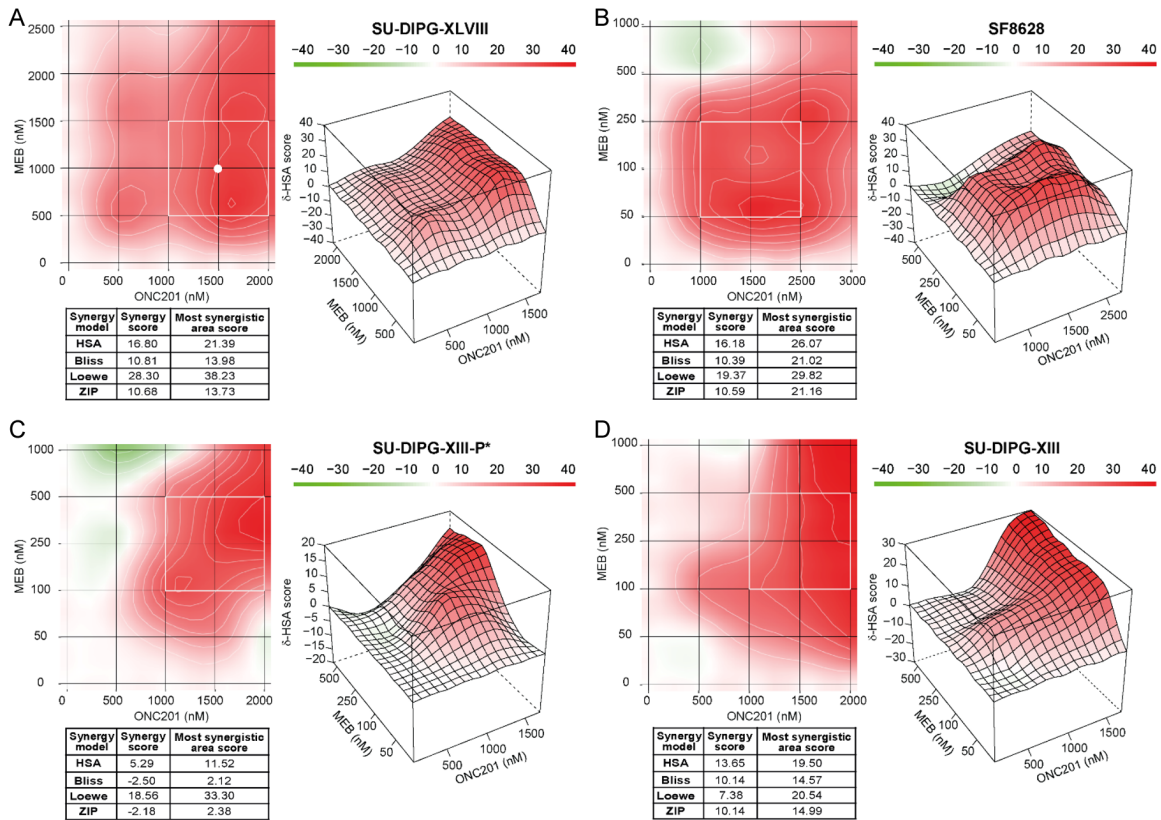


Figure 6. Comparison of the pharmacological interactions between MBZ and ONC201 calculated with different reference models confirms synergistic/additive effects of the combination in DMG cells. The combinatorial inhibitory effect of the MBZ and ONC201 combinations were analyzed by Synergy Finder from the individual viability measurements (shown in **Figure 5A**) in SU-DIPG-XLVIII (A) SF8628 (B), SU-DIPG-XIII-P* (C) and SU-DIPG-XIII (D). Each panel shows the 2D and 3D synergy maps as well as the table with synergy scores calculated with HSA, Bliss, Loewe and ZIP algorithms. The 2D and 3D synergy maps highlight synergistic and antagonistic dose regions in red and green colors, respectively. The white frame in each 2D plot represent the most synergistic area. The white dot in (A) indicates the drug combination used for the subsequent mechanistic studies.

(JHH-DIPG-1, SU-DIPG-XIII, SU-DIPG-XVII, SU-DIPG-XXV) [18]. However, no other cell-based studies beyond cytotoxicity assays were performed. We extended this panel of cultures by including six DMG cell lines so far uncharacterized for MBZ sensitivity, together with the previously reported SU-DIPG-XIII, used as a reference line. The IC_{50} values that we found fell in the range of the published values, and most importantly, of the concentrations attainable with the clinic dosages, thus highlighting the efficacy of MBZ at clinically relevant concentrations [40] against a vast array of DMG lines with different genetic backgrounds, including an H3 wild-type DMG model.

The antiproliferative MBZ properties were mediated by an arrest of DMG cells in the G2/M phase with a concomitant upregulation of the

key cell cycle regulators p21 and p27, which occurred regardless of the TP53-status of the cell lines, although they were more evident in those carrying wild-type TP53. In addition to the cytostatic effect, MBZ was able to reduce DMG cell survival by triggering apoptosis-related pathway. Our findings are in line with data from a wide variety of tumor models [12], in which mitotic arrest followed by caspase 3-mediated apoptotic cell death are among the main antitumor mechanisms induced by MBZ.

Cell cycle arrest at G2/M phase has been documented in acute lymphoblastic leukemia [11, 41], GBM [41], triple-negative breast cancer [42] and lung cancer [43, 44], whereas induction of the S-phase has inconsistently been reported [42]. In GBM cells, MBZ dose-dependently arrested the cell cycle at G2/M phase

Mebendazole against diffuse midline glioma

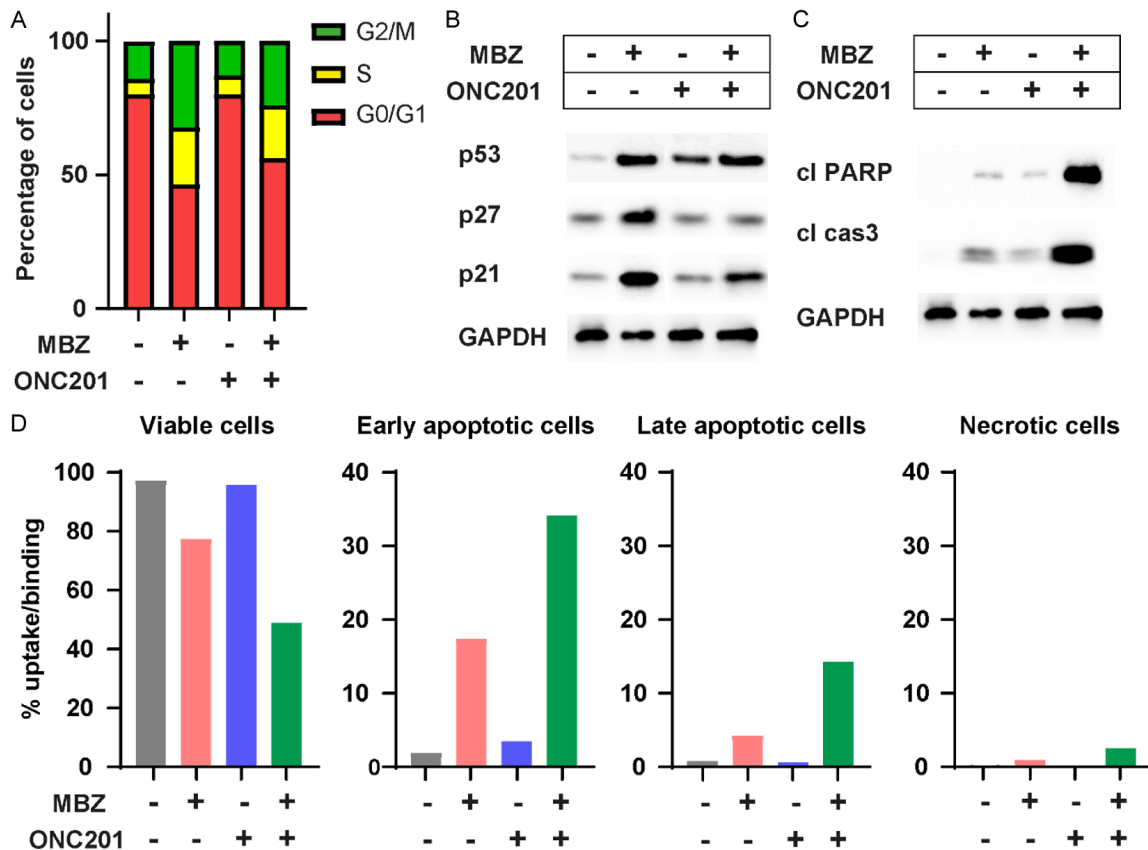


Figure 7. Cotreatment with ONC201 potentiates the pro-apoptotic effects of MBZ in DMG cell lines, while minimally affecting cell cycle distribution and checkpoint proteins. (A) Effects of both MBZ and ONC201, alone and in combination, on cell cycle distribution in SU-DIPG-XLVIII. Cells were treated with vehicle, MBZ (1 μ M), ONC201 (1.5 μ M) and both agents for 72 hours. The percentages of the total cell population in the different phases of the cell cycle were assessed by flow cytometry. (B, C) Western blot analysis of total lysates from SU-DIPG-XLVIII under the same conditions as in (A). Blots were probed with antibodies against regulatory proteins p53, p27 and p21 (B) and apoptosis markers (C). GAPDH was used as a loading control. (D) Flow cytometry analysis of SU-DIPG-XLVIII cells treated as in the above (A), stained with annexin V-FITC and PI.

through the p53/p21/cyclin B1 pathway [41]. However, this study explored only a short treatment up to 24 hours. Importantly, our data, in addition to confirming published findings in other tumor cell lines, including brain tumor cell lines, document a never-before-reported, long lasting cytokinetic effect of MBZ, up to 72 hours.

Although both cytostatic and cytotoxic effects of MBZ have been placed in the context of functional p53 [19], p53-mutated cells engage apoptosis as well. For example, both wild-type and mutant p53 melanoma cell lines were shown to be sensitive to MBZ [45]. By the same token, MBZ treatment caused post-translational p53 stabilization and the downstream expression of p21 and MDM2 in lung cancer

cell lines [40, 43]. However, p53-null lung cancer cells exposed to MBZ also apoptose through intrinsic and extrinsic pathways, as indicated by activation of caspase-9 and caspase-8. Similarly, MBZ growth-arrested ovarian cancer cell cultures regardless of their p53-status [46]. In our models, MBZ treatment was able to induce cell-cycle arrest and apoptosis regardless of TP53 status and protein modulation, suggesting that the antiproliferative/proapoptotic response to MBZ does not uniquely rely on p53 in DMG. These findings are of importance for DMG, where a relevant portion of tumors express mutant TP53 [4, 7, 47].

Because of its pleiotropic nature, it is likely that MBZ activates programmed cell death by inhibiting crucial prosurvival signaling, such as

Mebendazole against diffuse midline glioma

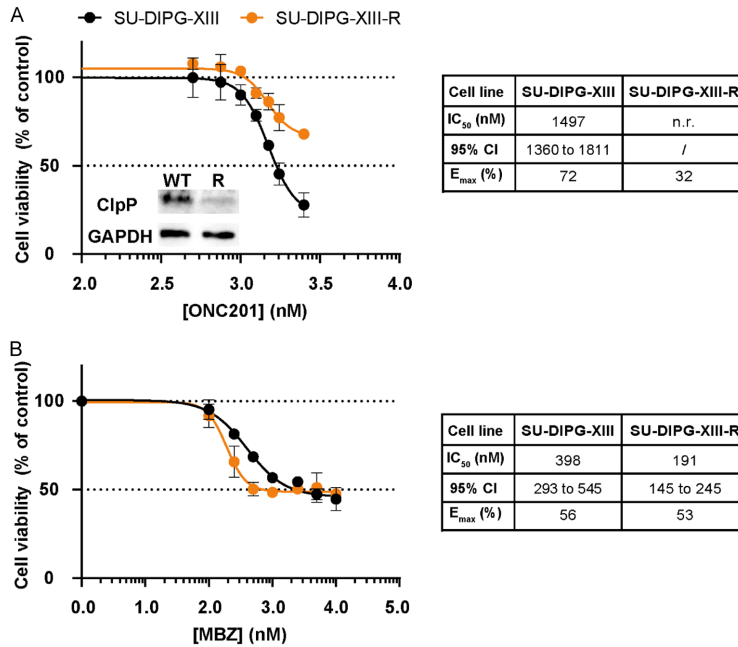


Figure 8. MBZ overcomes ONC201-resistance in SU-DIPG-XIII-R. (A, B) Graphic representations and tables of IC₅₀, 95% CI, and E_{max} of the antiproliferative effects of ONC201 (A) and MBZ (B) on paired ONC201-sensitive and -resistant SU-DIPG-XIII cell lines. Cell viability was measured by CTG assay after 72-hour drug exposure and expressed as percentage respect to vehicle-treated control cells. n.r.: not reached. *Inset* (A), western blot analysis of the expression of ClpP and of housekeeping GAPDH proteins in SU-DIPG-XIII (WT) and SU-DIPG-XIII-R (R).

PI3K/AKT and RAS/RAF/MEK/ERK, that play an important role in phosphorylating various apoptosis-regulating factors [11, 48-50]. In melanoma models, MBZ decreases the phosphorylation of MEK and ERK as well as that of the ERK downstream targets related to stress response and translation, including EIK1 and RSKs [51]. Dose-dependent hypophosphorylation of ERK1/2 and AKT by MBZ has also been documented in acute myeloid leukemia cells (AML), which suggests that the growth-inhibitory activity of MBZ on AML cells may be mediated in part via inhibition of these signaling [52]. In a more recent publication, MBZ-induced ROS accumulation in non small cell lung cancer cells inhibits STAT3 signaling and downregulates BCL-xl antiapoptotic protein, with concomitant upregulation of apoptotic markers [53]. MBZ' effects on the expression levels of antiapoptotic proteins, including XIAP and BCL2, have also been found in other models [54].

As for cell cycle progression, p21 has reportedly been documented as a key effector of the growth-inhibitory properties of MBZ in numer-

ous cancer cell lines. However, other cell cycle progression proteins, including MYC [55, 56], MYB [52], MAF [57], and cyclin D1 [49], to cite some, are down-regulated after MBZ challenging. Importantly, it has been shown that H3K27M drives cancer by epigenetic transcriptome remodelling, that ultimately leads to the activation of a RAS/MYC axis [58]. Therefore, MBZ targeting of these pathways may be a potential therapeutic option for H3K27M-driven cancers.

Until now monotherapies have unequivocally been unsuccessful in patients with a hard-to-treat disease such as DMG [33], except for ONC201 that has shown emerging clinical efficacy in early phase trials [34, 37], where a significant increase in median OS has been reported from historical 11.9 months to 21.7 months in ONC201-treated patients. However, children eventually succumb with some

even failing upfront treatment, indicating that intrinsic and/or acquired resistance to ONC201 occurs in DMG cells [59]. Combining drugs with different mechanisms of action for synergistic interactions optimizes treatment efficacy and safety [60], and could be particularly beneficial for DMGs that are characterized by a high degree of intratumoral and intertumoral heterogeneity [61, 62].

To build upon the preliminary promising efficacy of ONC201 and MBZ in the treatment of DMG, we explored the therapeutic potential of the combination of these two compounds. By using a dose-response matrix design, we found that combined treatments exerted a greater growth-inhibitory activity in four DMG lines compared with either single agent, resulting synergistic in two cultures and additive in the other two. Synergy between drugs vary upon several issues, such as cell-context and drug-class, introducing bias and reproducibility crisis in cancer drug combination discovery firstly in preclinical *in vivo* studies and secondly in the clinical setting [25, 60, 63]. Therefore, we vali-

dated the effects of the combination MBZ/ONC201 using four reference models developed on the basis of different assumptions, and, importantly, we found high consistency among all the interaction scores, further corroborating the combinatorial efficacy of these two compounds.

Mechanistically, the superior efficacy of MBZ/ONC201 cotreatment in DMG compared to single agents was mediated by enhanced apoptotic signaling rather than mitotic arrest, as evidenced by increased levels of activated caspase 3 and PARP cleavage, that exceeded by far the sum of single agent-induced upregulation of these cell death markers. This may suggest that the combination triggers two different apoptotic pathways, ONC201 relying on ClpP-dependent activation of the integrated stress response (ISR) and up-regulation of the TNF-related apoptosis-inducing ligand (TRAIL) pathway [64], while MBZ triggering activation of caspase-mediated intrinsic and extrinsic mitochondrial pathways [19]. Very importantly, we found the highest scores of sensitivity/additivity at concentrations of both MBZ and ONC201 [8] within the clinically achievable serum levels and regardless of the H3 K27 status of the cell lines. Although ONC201 is in clinical trials for DMG harboring the canonical H3K27M mutation, growing evidence suggests tumor-agnostic indication for ONC201 administration in patients, including wild-type H3 DMG.

To date, a few preclinical studies have found synergistic effects combining ONC201 with other agents, such as those targeting kinases [59], epigenetic modification enzymes [38], and proteasome [38]. Very recently, the combination of ONC201 and PTC596, an investigational antineoplastic small molecule that binds to the colchicine sites of tubulin similarly to MBZ, has demonstrated a strong synergistic growth-inhibitory effects on patient-derived DMG cultures, regardless of their H3K27M-status [65]. Together, these and our findings indicate that co-targeting tubulin and ClpP may be strategic for a patient population that continues to search for effective therapeutic strategies of combating difficult-to-treat disease.

MBZ's ability to overcome ONC201-resistance suggests that MBZ may block or bypass alternative mechanisms carried out by cancer cells to escape drug treatment. Different molecular

mechanisms may contribute to ONC201 resistance, including ClpP protein expression levels and/or mutation. Ectopic overexpression of ClpP sensitizes blood cancer cells to ONC201 [35], whereas loss of ClpP by CRISPR knockout confers resistance [59, 66]. ONC201 resistance has also been linked to a D190A mutation occurring in ONC201-selected cell lines [66]. In our DMG model, prolonged exposure to ONC201 determined a substantial decrease in ClpP protein level, consistent with the relationship between ONC201 sensitivity and the expression of its target ClpP. A plausible explanation for MBZ ability to circumvent the decrease sensitivity to ONC201 is the specific mechanism of action of each agent, targeting MBZ microtubules, while ONC201 being an activator of ClpP-mediated degradation of misfolded proteins. Our findings are in line with works by others, who documented that ONC201-resistant cells retain similar responsiveness to other drugs, such as adriamycin and vincristine [35], the latter inhibiting tubulin polymerizations as MBZ does.

A limitation of our study is the lack of preclinical *in vivo* validation, that hampers the assessment of the therapeutic potential of MBZ in a more reliable environment, where the complex tumor architecture along with pharmacokinetics factors may impact on drug delivery to the tumor sites and the response to drug. This limitation is partly due to the very limited number of tumorigenic DMG cell lines and their very slow rate of growth *in vivo*, which makes preclinical models very cumbersome. We tried to compensate for this limitation by using a large panel of genetically different DMG cell lines, most of which grow in 3D cultures as floating neurospheres, the *in vitro* models that more reliably resemble *in vivo* tumors [67]. In addition, literature data from preclinical and clinical studies document high blood-brain-barrier permeability to MBZ and ONC201, suggesting that our results *in vitro* may likely translate to *in vivo* setting.

Active research is currently underway to further our understanding of MBZ anticancer mechanisms of action as well as of its clinical efficacy. Although MBZ demonstrates potent effects as a potential new low-toxicity therapeutic for DMG, further investigations in DMG *in vivo* models are warranted to confirm the preclinical anti-neoplastic activity of MBZ and its safety in

combination with other drugs for future translation into a clinical setting.

Conclusion

To the best of our knowledge, this study is the first to thoroughly investigate the anticancer activity of repurposed MBZ in a panel of DMG lines, both as monotherapy and in combination with ONC201. Our study provides the cellular and molecular insights for a novel potential combination strategy that, joining together two low-toxicity, preclinically effective, anticancer compounds, exerts synergistic growth-inhibitory and pro-apoptotic activity in H3K27-mutated and H3-wild-type DMG cell lines. In addition to its chemosensitizing activity to ONC201, we highlight the preclinical potential of MBZ as a second line treatment opportunity in advanced DMG setting.

Acknowledgements

We thank Dr. Michelle Monje (Department of Neurology and Neurological Sciences, Stanford University, Stanford, CA, USA) for giving us the patient-derived DMG cell lines. This study was supported by Fondazione per l'Oncologia Pediatrica (FOP) and "Finanziato dall'Unione europea - Next Generation EU - PNRR M6C2 - Investimento 2.1 Valorizzazione e potenziamento della ricerca biomedica del SSN", Grant PNRR-TR1-2023-12378160, European Union.

Disclosure of conflict of interest

None.

Address correspondence to: Tiziana Servidei, Pediatric Oncology Unit, Department of Woman and Child Health Sciences and Public Health, Fondazione Policlinico Universitario A. Gemelli IRCCS, Largo A. Gemelli, 8, 00168 Rome, Italy. E-mail: tiziana.servidei@guest.policlinicogemelli.it

References

- [1] Louis D, Perry A, Wesseling P, Brat D, Cree I, Figarella-Branger D, Hawkins C, Ng H, Pfister S, Reifenberger G, Soffietti R, Deimling A and Ellison D. The 2021 WHO classification of tumors of the central nervous system: a summary. *Neuro Oncol* 2021; 23: 1231-1251.
- [2] Pfister SM, Reyes-Múgica M, Chan JKC, Hasle H, Lazar AJ, Rossi S, Ferrari A, Jarzembowski JA, Pritchard-Jones K, Hill DA, Jacques TS,

Wesseling P, López Terrada DH, von Deimling A, Kratz CP, Cree IA and Alaggio R. A summary of the inaugural WHO classification of pediatric tumors: transitioning from the optical into the molecular era. *Cancer Discov* 2022; 12: 331-355.

- [3] Jackson ER, Persson ML, Fish CJ, Findlay IJ, Mueller S, Nazarian J, Hulleman E, van der Lugt J, Duchatel RJ and Dun MD. A review of current therapeutics targeting the mitochondrial protease ClpP in diffuse midline glioma, H3 K27-altered. *Neuro Oncol* 2024; 26: S136-S154.
- [4] Damodharan S, Abbott A, Kellar K, Zhao Q and Dey M. Molecular characterization and treatment approaches for pediatric H3 K27-altered diffuse midline glioma: integrated systematic review of individual clinical trial participant data. *Cancers (Basel)* 2023; 15: 3478.
- [5] Hoffman LM, Veldhuijzen van Zanten SEM, Colditz N, Baugh J, Chaney B, Hoffmann M, Lane A, Fuller C, Miles L, Hawkins C, Bartels U, Bouffet E, Goldman S, Leary S, Foreman NK, Packer R, Warren KE, Broniscer A, Kieran MW, Minturn J, Comito M, Broxson E, Shih CS, Khatua S, Chintagumpala M, Carret AS, Escorza NY, Hassall T, Ziegler DS, Gottardo N, Dholaria H, Doughman R, Benesch M, Drissi R, Nazarian J, Jabado N, Boddaert N, Varlet P, Giraud G, Castel D, Puget S, Jones C, Hulleman E, Modena P, Giagnacovo M, Antonelli M, Pietsch T, Gielen GH, Jones DTW, Sturm D, Pfister SM, Gerber NU, Grotzer MA, Pfaff E, von Bueren AO, Hargrave D, Solanki GA, Jadrijevic Cvrlje F, Kaspers GJL, Vandertop WP, Grill J, Bailey S, Biassoni V, Massimino M, Calmon R, Sanchez E, Bison B, Warmuth-Metz M, Leach J, Jones B, van Vuurden DG, Kramm CM and Fouladi M. Clinical, radiologic, pathologic, and molecular characteristics of long-term survivors of diffuse intrinsic pontine glioma (dipg): a collaborative report from the international and European society for pediatric oncology DIPG registries. *J Clin Oncol* 2018; 36: 1963-1972.
- [6] Bayliss J, Mukherjee P, Lu C, Jain SU, Chung C, Martinez D, Sabari B, Margol AS, Panwalkar P, Parolia A, Pekmezci M, McEachin RC, Cieslik M, Tamrazi B, Garcia BA, La Rocca G, Santi M, Lewis PW, Hawkins C, Melnick A, David Allis C, Thompson CB, Chinnaiyan AM, Judkins AR and Venneti S. Lowered H3K27me3 and DNA hypomethylation define poorly prognostic pediatric posterior fossa ependymomas. *Sci Transl Med* 2016; 8: 366ra161.
- [7] Findlay IJ, De Luliis GN, Duchatel RJ, Jackson ER, Vitanza NA, Cain JE, Waszak SM and Dun MD. Pharmacoproteogenomic profiling of pediatric diffuse midline glioma to inform future treatment strategies. *Oncogene* 2022; 41: 461-475.

Mebendazole against diffuse midline glioma

- [8] Servidei T, Sgambato A, Lucchetti D, Navarra P and Ruggiero A. Drug repurposing in pediatric brain tumors: posterior fossa ependymoma and diffuse midline glioma under the looking glass. *Front Biosci (Landmark Ed)* 2023; 28: 77.
- [9] Xia Y, Sun M, Huang H and Jin WL. Drug repurposing for cancer therapy. *Sig Transduct Target Ther* 2024; 9: 92.
- [10] Bai RY, Staedtke V, Aprhys CM, Gallia GL and Riggins GJ. Antiparasitic mebendazole shows survival benefit in 2 preclinical models of glioblastoma multiforme. *Neuro Oncol* 2011; 13: 974-982.
- [11] Golla U, Patel S, Shah N, Talamo S, Bhalodia R, Claxton D, Dovat S and Sharma A. From deworming to cancer therapy: benzimidazoles in hematological malignancies. *Cancers (Basel)* 2024; 16: 3454.
- [12] Meco D, Attinà G, Mastrangelo S, Navarra P and Ruggiero A. Emerging perspectives on the antiparasitic mebendazole as a repurposed drug for the treatment of brain cancers. *Int J Mol Sci* 2023; 24: 1334.
- [13] Jornet D, Bosca F, Andreu JM, Domingo LR, Tormos R and Miranda MA. Analysis of mebendazole binding to its target biomolecule by laser flash photolysis. *J Photochem Photobiol B* 2016; 155: 1-6.
- [14] De Witt M, Gamble A, Hanson D, Markowitz D, Powell C, Al Dimassi S, Atlas M, Boockvar J, Ruggieri R and Symons M. Repurposing mebendazole as a replacement for vincristine for the treatment of brain tumors. *Mol Med* 2017; 23: 50-56.
- [15] Braithwaite PA, Roberts MS, Allan RJ and Watson TR. Clinical pharmacokinetics of high dose mebendazole in patients treated for cystic hydatid disease. *Eur J Clin Pharmacol* 1982; 22: 161-169.
- [16] Bodhinayake I, Symons M and Boockvar JA. Repurposing mebendazole for the treatment of medulloblastoma. *Neurosurgery* 2015; 76: N15-16.
- [17] Shen M, Asawa R, Zhang YQ, Cunningham E, Sun H, Tropsha A, Janzen WP, Muratov EN, Capuzzi SJ, Farag S, Jadhav A, Blatt J, Simeonov A and Martinez NJ. Quantitative high-throughput phenotypic screening of pediatric cancer cell lines identifies multiple opportunities for drug repurposing. *Oncotarget* 2017; 9: 4758-4772.
- [18] Lin GL, Wilson KM, Ceribelli M, Stanton BZ, Woo PJ, Kreimer S, Qin EY, Zhang X, Lennon J, Nagaraja S, Morris PJ, Quezada M, Gillespie SM, Duvéau DY, Michalowski AM, Shinn P, Guha R, Ferrer M, Klumpp-Thomas C, Michael S, McKnight C, Minhas P, Itkin Z, Raabe EH, Chen L, Ghanem R, Geraghty AC, Ni L, Andreasson KI, Vitanza NA, Warren KE, Thomas CJ and Monje M. Therapeutic strategies for diffuse midline glioma from high-throughput combination drug screening. *Sci Transl Med* 2019; 11: eaaw0064.
- [19] Guerini AE, Triggiani L, Maddalo M, Bonù ML, Frassine F, Baiguini A, Alghisi A, Tomasini D, Borghetti P, Pasinetti N, Bresciani R, Magrini SM and Buglione M. Mebendazole as a candidate for drug repurposing in oncology: an extensive review of current literature. *Cancers (Basel)* 2019; 11: 1284.
- [20] Nath J, Paul R, Ghosh SK, Paul J, Singha B and Debnath N. Drug repurposing and relabeling for cancer therapy: emerging benzimidazole antihelminthics with potent anticancer effects. *Life Sci* 2020; 258: 118189.
- [21] Mueller S, Jain P, Liang WS, Kilburn L, Kline C, Gupta N, Panditharatna E, Magge SN, Zhang B, Zhu Y, Crawford JR, Banerjee A, Nazemi K, Packer RJ, Petritsch CK, Truffaux N, Roos A, Nasser S, Phillips JJ, Solomon D, Molinaro A, Waanders AJ, Byron SA, Berens ME, Kuhn J, Nazarian J, Prados M and Resnick AC. A pilot precision medicine trial for children with diffuse intrinsic pontine glioma-PNOC003: a report from the Pacific pediatric neuro-oncology consortium. *Int J Cancer* 2019; 145: 1889-1901.
- [22] Gojo J, Pavelka Z, Zapletalova D, Schmook MT, Mayr L, Madlener S, Kyr M, Vejmelkova K, Smrcka M, Czech T, Dorfer C, Skotakova J, Azizi AA, Chocholous M, Reisinger D, Lastovicka D, Valik D, Haberler C, Peyrl A, Noskova H, Pál K, Jezova M, Veselska R, Kozakova S, Slaby O, Slavic I and Sterba J. Personalized treatment of H3K27M-mutant pediatric diffuse gliomas provides improved therapeutic opportunities. *Front Oncol* 2019; 9: 1436.
- [23] Chou TC and Talalay P. Quantitative analysis of dose-effect relationships: the combined effects of multiple drugs or enzyme inhibitors. *Adv Enzyme Regul* 1984; 22: 27-55.
- [24] Ianevski A, Giri AK and Aittokallio T. Synergy-Finder 3.0: an interactive analysis and consensus interpretation of multi-drug synergies across multiple samples. *Nucleic Acids Res* 2022; 50: W739-W743.
- [25] Yadav B, Wennerberg K, Aittokallio T and Tang J. Searching for drug synergy in complex dose-response landscapes using an interaction potency model. *Comput Struct Biotechnol J* 2015; 13: 504-513.
- [26] Qin EY, Cooper DD, Abbott KL, Lennon J, Nagaraja S, Mackay A, Jones C, Vogel H, Jackson PK and Monje M. Neural precursor-derived pleiotrophin mediates subventricular zone invasion by glioma. *Cell* 2017; 170: 845-859, e19.

Mebendazole against diffuse midline glioma

- [27] Sinha S, Huang MS, Mikos G, Bedi Y, Soto L, Lensch S, Ayushman M, Bintu L, Bhutani N, Heilshorn SC and Yang F. Laminin-associated integrins mediate diffuse intrinsic pontine glioma infiltration and therapy response within a neural assembloid model. *Acta Neuropathol Commun* 2024; 12: 71.
- [28] Berenguer-Daizé C, Astorgues-Xerri L, Odore E, Cayol M, Cvitkovic E, Noel K, Bekradda M, MacKenzie S, Rezai K, Lokiec F, Riveiro ME and Ouafik L. OTX015 (MK-8628), a novel BET inhibitor, displays in vitro and in vivo antitumor effects alone and in combination with conventional therapies in glioblastoma models. *Int J Cancer* 2016; 139: 2047-2055.
- [29] Gallia GL, Holdhoff M, Brem H, Joshi AD, Hann CL, Bai RY, Staedtke V, Blakeley JO, Sengupta S, Jarrell TC, Wollett J, Szajna K, Helie N, Mattox AK, Ye X, Rudek MA and Riggins GJ. Mebendazole and temozolomide in patients with newly diagnosed high-grade gliomas: results of a phase 1 clinical trial. *Neurooncol Adv* 2021; 3: vdaa154.
- [30] Cassim A, Dun MD, Gallego-Ortega D and Valdes-Mora F. EZHIP's role in diffuse midline glioma: echoes of oncohistones? *Trends Cancer* 2024; 10: 1095-1105.
- [31] Maclaine NJ and Hupp TR. The regulation of p53 by phosphorylation: a model for how distinct signals integrate into the p53 pathway. *Aging* 2009; 1: 490.
- [32] Meitinger F, Belal H, Davis RL, Martinez MB, Shiau AK, Oegema K and Desai A. Control of cell proliferation by memories of mitosis. *Science* 2024; 383: 1441-1448.
- [33] Duchatel RJ, Jackson ER, Parackal SG, Kiltchewskij D, Findlay IJ, Mannan A, Staudt DE, Thomas BC, Germon ZP, Latenser S, Kearney PS, Jamaluddin MFB, Douglas AM, Beitaki T, McEwen HP, Persson ML, Hocke EA, Jain V, Aksu M, Manning EE, Murray HC, Verrills NM, Sun CX, Daniel P, Vilain RE, Skerrett-Byrne DA, Nixon B, Hua S, de Bock CE, Colino-Sanguino Y, Valdes-Mora F, Tsoli M, Ziegler DS, Cairns MJ, Raabe EH, Vitanza NA, Hulleman E, Phoenix TN, Koschmann C, Alvaro F, Dayas CV, Tinkle CL, Wheeler H, Whittle JR, Eisenstat DD, Firestein R, Mueller S, Valvi S, Hansford JR, Ashley DM, Gregory SG, Kilburn LB, Nazarian J, Cain JE and Dun MD. PI3K/mTOR is a therapeutically targetable genetic dependency in diffuse intrinsic pontine glioma. *J Clin Invest* 2024; 134: e170329.
- [34] Arrillaga-Romany I, Gardner SL, Odia Y, Aguilera D, Allen JE, Batchelor T, Butowski N, Chen C, Cloughesy T, Cluster A, de Groot J, Dixit KS, Graber JJ, Haggiagi AM, Harrison RA, Kheradpour A, Kilburn L, Kurz SC, Lu G, MacDonald TJ, Mehta M, Melemed AS, Nghiemphu PL, Ramage SC, Shonka N, Sumrall A, Tarapore R, Taylor L, Umemura Y and Wen PY. ONC201 (Dordaviprone) in recurrent H3 K27M-mutant diffuse midline glioma. *J Clin Oncol* 2024; 42: 1542-1552.
- [35] Ishizawa J, Zarabi SF, Davis RE, Halgas O, Nii T, Jitkova Y, Zhao R, St-Germain J, Heese LE, Egan G, Ruvolo VR, Barghout SH, Nishida Y, Hurren R, Ma W, Gronda M, Link T, Wong K, Mabanglo M, Kojima K, Borthakur G, MacLean N, Ma MCJ, Leber AB, Minden MD, Houry W, Kantarjian H, Stogniew M, Raught B, Pai EF, Schimmer AD and Andreeff M. Mitochondrial ClpP-mediated proteolysis induces selective cancer cell lethality. *Cancer Cell* 2019; 35: 721-737, e9.
- [36] Ianevski A, He L, Aittokallio T and Tang J. SynergyFinder: a web application for analyzing drug combination dose-response matrix data. *Bioinformatics* 2017; 33: 2413-2415.
- [37] Venneti S, Kawakibi AR, Ji S, Waszak SM, Sweha SR, Mota M, Pun M, Deogharkar A, Chung C, Tarapore RS, Ramage S, Chi A, Wen PY, Arrillaga-Romany I, Batchelor TT, Butowski NA, Sumrall A, Shonka N, Harrison RA, de Groot J, Mehta M, Hall MD, Daghistani D, Cloughesy TF, Ellingson BM, Beccaria K, Varlet P, Kim MM, Umemura Y, Garton H, Franson A, Schwartz J, Jain R, Kachman M, Baum H, Burant CF, Mottl SL, Cartaxo RT, John V, Messinger D, Qin T, Peterson E, Sajjakulnukit P, Ravi K, Waugh A, Walling D, Ding Y, Xia Z, Schwendeman A, Hawes D, Yang F, Judkins AR, Wahl D, Lyssiotis CA, de la Nava D, Alonso MM, Eze A, Spitzer J, Schmidt SV, Duchatel RJ, Dun MD, Cain JE, Jiang L, Stopka SA, Baquer G, Regan MS, Filbin MG, Agar NYR, Zhao L, Kumar-Sinha C, Mody R, Chinnaiyan A, Kurokawa R, Pratt D, Yadav VN, Grill J, Kline C, Mueller S, Resnick A, Nazarian J, Allen JE, Odia Y, Gardner SL and Koschmann C. Clinical efficacy of ONC201 in H3K27M-mutant diffuse midline gliomas is driven by disruption of integrated metabolic and epigenetic pathways. *Cancer Discov* 2023; 13: 2370-2393.
- [38] Borsuk R, Zhou L, Chang WI, Zhang Y, Sharma A, Prabhu VV, Tapinos N, Lulla RR and El-Deiry WS. Potent preclinical sensitivity to imipridone-based combination therapies in oncohistone H3K27M-mutant diffuse intrinsic pontine glioma is associated with induction of the integrated stress response, TRAIL death receptor DR5, reduced ClpX and apoptosis. *Am J Cancer Res* 2021; 11: 4607-4623.
- [39] Xia Y, Sun M, Huang H and Jin WL. Drug repurposing for cancer therapy. *Signal Transduct Target Ther* 2024; 9: 92.
- [40] Pantziarka P, Bouche G, Meheus L, Sukhatme V and Sukhatme VP. Repurposing drugs in on-

Mebendazole against diffuse midline glioma

- cology (ReDO)-mebendazole as an anti-cancer agent. *Ecancermedicalsecience* 2014; 8: 443.
- [41] Ren LW, Li W, Zheng XJ, Liu JY, Yang YH, Li S, Zhang S, Fu WQ, Xiao B, Wang JH and Du GH. Benzimidazoles induce concurrent apoptosis and pyroptosis of human glioblastoma cells via arresting cell cycle. *Acta Pharmacol Sin* 2022; 43: 194-208.
- [42] Choi HS, Ko YS, Jin H, Kang KM, Ha IB, Jeong H, Song HN, Kim HJ and Jeong BK. Anticancer effect of benzimidazole derivatives, especially mebendazole, on triple-negative breast cancer (TNBC) and radiotherapy-resistant TNBC in vivo and in vitro. *Molecules* 2021; 26: 5118.
- [43] Mukhopadhyay T, Sasaki J, Ramesh R and Roth JA. Mebendazole elicits a potent antitumor effect on human cancer cell lines both in vitro and in vivo. *Clin Cancer Res* 2002; 8: 2963-2969.
- [44] Sasaki J, Ramesh R, Chada S, Gomyo Y, Roth JA and Mukhopadhyay T. The anthelmintic drug mebendazole induces mitotic arrest and apoptosis by depolymerizing tubulin in non-small cell lung cancer cells. *Mol Cancer Ther* 2002; 1: 1201-1209.
- [45] Doudican N, Rodriguez A, Osman I and Orlov SJ. Mebendazole induces apoptosis via Bcl-2 inactivation in chemoresistant melanoma cells. *Mol Cancer Res* 2008; 6: 1308-1315.
- [46] Elayapillai S, Ramraj S, Benbrook DM, Bieniasz M, Wang L, Pathuri G, Isingizwe ZR, Kennedy AL, Zhao YD, Lightfoot S, Hunsucker LA and Gunderson CC. Potential and mechanism of mebendazole for treatment and maintenance of ovarian cancer. *Gynecol Oncol* 2021; 160: 302-311.
- [47] Pathania M, De Jay N, Maestro N, Harutyunyan AS, Nitaraska J, Pahlavan P, Henderson S, Mikael LG, Richard-Londt A, Zhang Y, Costa JR, Hébert S, Khazaei S, Ibrahim NS, Herrero J, Riccio A, Albrecht S, Ketteler R, Brandner S, Kleinman CL, Jabado N and Salomoni P. H3.3K27M cooperates with Trp53 loss and PDGFRA gain in mouse embryonic neural progenitor cells to induce invasive high-grade gliomas. *Cancer Cell* 2017; 32: 684-700, e9.
- [48] Liu F, Yang X, Geng M and Huang M. Targeting ERK, an Achilles' Heel of the MAPK pathway, in cancer therapy. *Acta Pharm Sin B* 2018; 8: 552-562.
- [49] Younis NS, Ghanim AMH and Saber S. Mebendazole augments sensitivity to sorafenib by targeting MAPK and BCL-2 signalling in n-nitrosodiethylamine-induced murine hepatocellular carcinoma. *Sci Rep* 2019; 9: 19095.
- [50] McCubrey JA, Steelman LS, Chappell WH, Abrams SL, Wong EWT, Chang F, Lehmann B, Terrian DM, Milella M, Tafuri A, Stivala F, Libra M, Basccke J, Evangelisti C, Martelli AM and Franklin RA. Roles of the Raf/MEK/ERK pathway in cell growth, malignant transformation and drug resistance. *Biochim Biophys Acta* 2007; 1773: 1263-1284.
- [51] Simbulan-Rosenthal CM, Dakshanamurthy S, Gaur A, Chen YS, Fang HB, Abdussamad M, Zhou H, Zapas J, Calvert V, Petricoin EF, Atkins MB, Byers SW and Rosenthal DS. The repurposed anthelmintic mebendazole in combination with trametinib suppresses refractory NRASQ61K melanoma. *Oncotarget* 2017; 8: 12576-12595.
- [52] He L, Shi L, Du Z, Huang H, Gong R, Ma L, Chen L, Gao S, Lyu J and Gu H. Mebendazole exhibits potent anti-leukemia activity on acute myeloid leukemia. *Exp Cell Res* 2018; 369: 61-68.
- [53] Liang Z, Chen Q, Pan L, She X and Chen T. Mebendazole induces apoptosis and inhibits migration via the reactive oxygen species-mediated STAT3 signaling downregulation in non-small cell lung cancer. *J Thorac Dis* 2024; 16: 1412-1423.
- [54] Doudican NA, Byron SA, Pollock PM and Orlov SJ. XIAP downregulation accompanies mebendazole growth inhibition in melanoma xenografts. *Anticancer Drugs* 2013; 24: 181-188.
- [55] da Silva EL, Mesquita FP, Pinto LC, Gomes BPS, de Oliveira EHC, Burbano RMR, Moraes MEA de, de Souza PFN and Montenegro RC. Transcriptome analysis displays new molecular insights into the mechanisms of action of Mebendazole in gastric cancer cells. *Comput Biol Med* 2025; 184: 109415.
- [56] Zhang F, Li Y, Zhang H, Huang E, Gao L, Luo W, Wei Q, Fan J, Song D, Liao J, Zou Y, Liu F, Liu J, Huang J, Guo D, Ma C, Hu X, Li L, Qu X, Chen L, Yu X, Zhang Z, Wu T, Luu HH, Haydon RC, Song J, He TC and Ji P. Anthelmintic mebendazole enhances cisplatin's effect on suppressing cell proliferation and promotes differentiation of head and neck squamous cell carcinoma (HNSCC). *Oncotarget* 2017; 8: 12968-12982.
- [57] Chen XH, Xu YJ, Wang XG, Lin P, Cao BY, Zeng YY, Wang Q, Zhang ZB, Mao XL and Zhang T. Mebendazole elicits potent antimyeloma activity by inhibiting the USP5/c-Maf axis. *Acta Pharmacol Sin* 2019; 40: 1568-1577.
- [58] Pajovic S, Siddaway R, Bridge T, Sheth J, Rakopoulos P, Kim B, Ryall S, Agnihotri S, Phillips L, Yu M, Li C, Milos S, Patel P, Srikanthan D, Huang A and Hawkins C. Epigenetic activation of a RAS/MYC axis in H3.3K27M-driven cancer. *Nat Commun* 2020; 11: 6216.
- [59] Jackson ER, Duchatel RJ, Staudt DE, Persson ML, Mannan A, Yadavilli S, Parackal S, Game S, Chong WC, Jayasekara WSN, Grand ML, Kearney PS, Douglas AM, Findlay IJ, Germon

Mebendazole against diffuse midline glioma

- ZP, McEwen HP, Beitaki TS, Patabendige A, Skerrett-Byrne DA, Nixon B, Smith ND, Day B, Manoharan N, Nagabushan S, Hansford JR, Govender D, McCowage GB, Firestein R, Howlett M, Endersby R, Gottardo NG, Alvaro F, Waszak SM, Larsen MR, Colino-Sanguino Y, Valdes-Mora F, Rakotomalala A, Meignan S, Pasquier E, André N, Hulleman E, Eisenstat DD, Vitanza NA, Nazarian J, Koschmann C, Mueller S, Cain JE and Dun MD. *ONC201 in combination with paxalisib for the treatment of H3K27-altered diffuse midline glioma. Cancer Res* 2023; **OF1-OF17**.
- [60] Calzetta L, Page C, Matera MG, Cazzola M and Rogliani P. Drug-drug interactions and synergy: from pharmacological models to clinical application. *Pharmacol Rev* 2024; **76: 1159-1220**.
- [61] Filbin MG, Tirosh I, Hovestadt V, Shaw ML, Escalante LE, Mathewson ND, Neftel C, Frank N, Pelton K, Hebert CM, Haberler C, Yizhak K, Gojo J, Egervari K, Mount C, van Galen P, Bonal DM, Nguyen QD, Beck A, Sinai C, Czech T, Dorfer C, Goumnerova L, Lavarino C, Carcaboso AM, Mora J, Mylvaganam R, Luo CC, Peyrl A, Popović M, Azizi A, Batchelor TT, Frosch MP, Martinez-Lage M, Kieran MW, Bandopadhyay P, Beroukhim R, Fritsch G, Getz G, Rozenblatt-Rosen O, Wucherpfeffig KW, Louis DN, Monje M, Slavic I, Ligon KL, Golub TR, Regev A, Bernstein BE and Suvà ML. Developmental and oncogenic programs in H3K27M gliomas dissected by single-cell RNA-seq. *Science* 2018; **360: 331-335**.
- [62] Murdaugh RL and Anastas JN. Applying single cell multi-omic analyses to understand treatment resistance in pediatric high grade glioma. *Front Pharmacol* 2023; **14: 1002296**.
- [63] Ianevski A, He L, Aittokallio T and Tang J. SynergyFinder: a web application for analyzing drug combination dose-response matrix data. *Bioinformatics* 2020; **36: 2645**.
- [64] Endo Greer Y and Lipkowitz S. *ONC201: Stressing tumors to death. Sci Signal* 2016; **9: fs1**.
- [65] Deligne C, Tourbez A, Bénard F, Meyer S, Curt A, Ganesello M, Hamadou M, Clavier L, Coquet C, Bocquet C, Tomine J, Diot T, Paraquindes H, Marcel V, Berthelot C, Engel J, Rochet I, Barritault M, Savary C, Gadot N, Attignon V, Carrere M, Billaud M, Dutour A, Cordier-Bussat M, Beuriat PA, Szathmari A, Di Rocco F, Blay JY, Tiberi L, Vasiljevic A, Meyronet D, Castets M, Leblond P and Broutier L. Establishing a living biobank of pediatric high-grade glioma and ependymoma suitable for cancer pharmacology. *Neuro Oncol* 2025; **noaf007**.
- [66] Jacques S, van der Sloot AM, C Huard C, Coulombe-Huntington J, Tsao S, Tollis S, Bertomeu T, Culp EJ, Pallant D, Cook MA, Bonneil E, Thibault P, Wright GD and Tyers M. Imipridone anticancer compounds ectopically activate the clpp protease and represent a new scaffold for antibiotic development. *Genetics* 2020; **214: 1103-1120**.
- [67] Fontoura JC, Viezzer C, Dos Santos FG, Ligabue RA, Weinlich R, Puga RD, Antonow D, Severino P and Bonorino C. Comparison of 2D and 3D cell culture models for cell growth, gene expression and drug resistance. *Mater Sci Eng C Mater Biol Appl* 2020; **107: 110264**.